NASA Space Laser Technology

Michael A. Krainak

Representing the work of hundreds of people

NASA Goddard Space Flight Center
Laser & Electro-Optics Branch
Code 554

September 15, 2014

NASA Space Laser Technology
AGENDA

I. Overview of existing and near-term space laser systems

II. Monolithic solid state lasers

I. Future missions

Space Laser Altimetry Instruments

Apollo - moon
NASA (1971-1972)
Ruby lasers,
5,000 shots

Clementine - moon
LLNL/NRL (1994)
Nd:YAG laser,
~72,000 shots

NEAR/NLR - Eros
JHU/APL (1996-2001)
Nd:YAG laser,
11 million shots

MGS/MOLA - Mars
NASA GSFC (1996 -2000)
Nd:YAG laser,
670 million shots

ICESat/GLAS - Earth
NASA GSFC (2003-2010)
Nd:YAG laser
1.98 billion shots

MESSENGER/MLA - Mercury
NASA GSFC (2004-present)
Nd:YAG laser,
35 Million shots to date

LRO/LOLA - moon
NASA GSFC (2008-present)
Nd:YAG laser,
400 million shots to date

SELENE/LALT - moon
Japan (2007-2009)
Nd:YAG laser

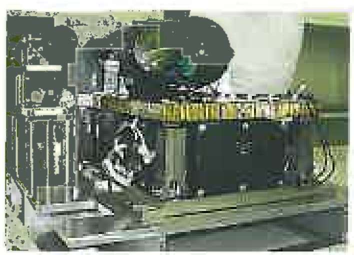

Chang'E - moon
China (2007-present)
Nd:YAG laser

Chandrayaan/LLRI - moon
India (2008-2010)
Nd:YAG laser,

Current and future missions......

BELA/BepiColumbo – Mercury, **ESA** (launch in 2016) Nd:YAG laser

GEDI – Earth NASA GSFC (launch in 2019) Nd:YAG lasers

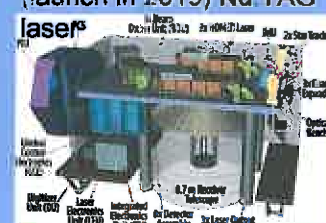

ICESat-2/ATLAS – Earth
NASA GSFC (launch in 2017)
Nd:YVO_4 laser

Geoscience Laser Altimeter System (GLAS)

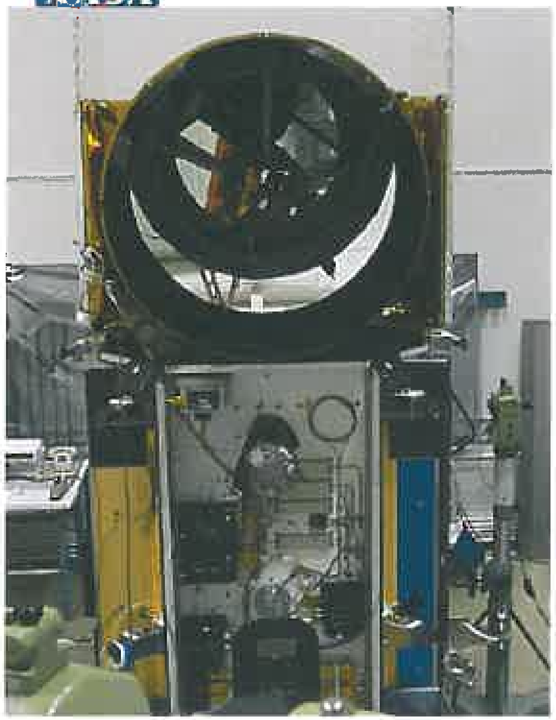

GLAS Instrument

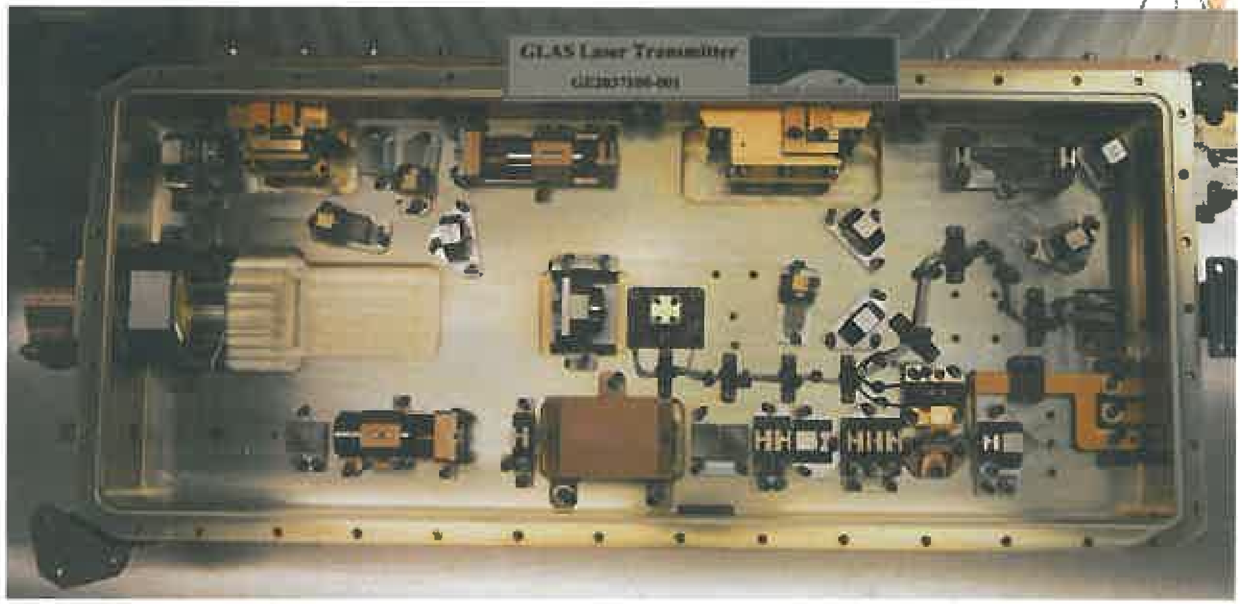

GLAS Laser Transmitter

Instrument	**GLAS**	
Mission	ICESat	
Laser type	Cr:Nd:YAG, passive q-switch	
Laser Architecture	Porro-Mirror resonator passively Q-switched with two stage amplifiers	
# of lasers	3	
Laser Wavelength	$\lambda 1$ 1064.5 nm $\pm$ 100 pm	$\lambda 2$ 532.2 nm $\pm$ 50 pm($\leq$ 15 pm single shot)
Laser pulse energy	$\lambda 1 = 75$ mJ	$\lambda 2 = 35$ mJ
Laser Pulse Repetition Rate	40 $\pm$ 0.1 Hz	
Laser Pulsewidth	$\leq$ 6 ns	
Laser Beam quality	TEM00	
Laser Divergence	110 μrad (+23, -10)	

Mercury Laser Altimeter (MLA)

MLA Laser Transmitter – derivative of GLAS laser MOPA design, 8Hz, 20 mJ
Detector – same as GLAS, SiAPD

Lunar Orbiter Laser Altimeter (LOLA)

First multi-beam Space-based Altimeter Instrument

Laser Transmitter – Derivative of GLAS Master Oscillator,
Two lasers on a single bench for redundancy
Receiver – Same as GLAS, MLA - SiAPD

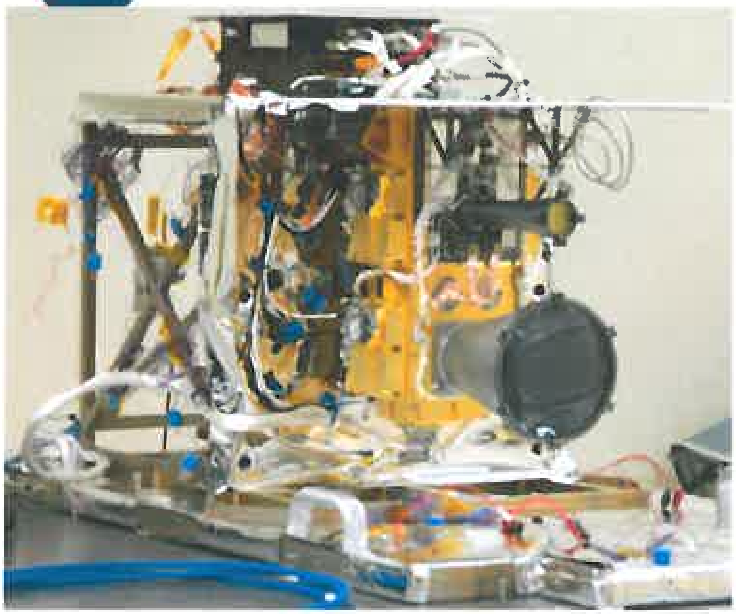

Fiber Pattern at

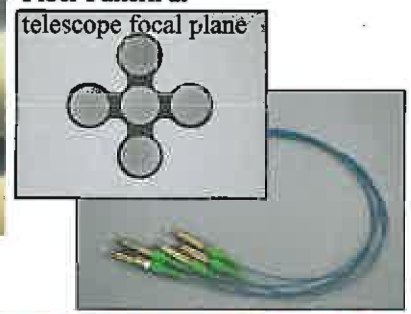

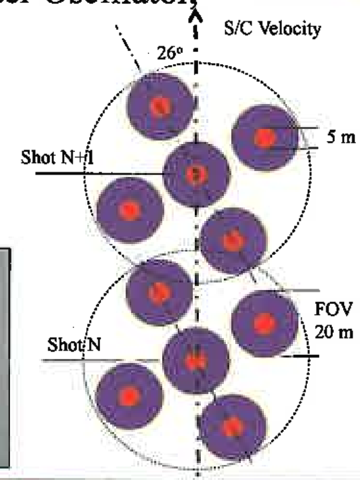

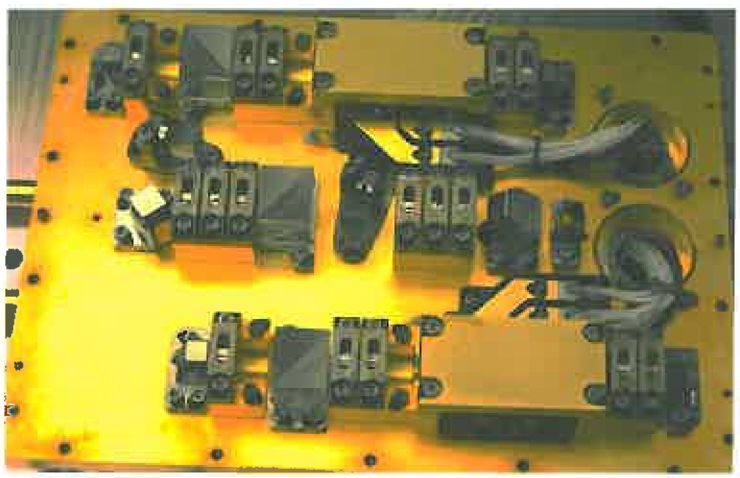

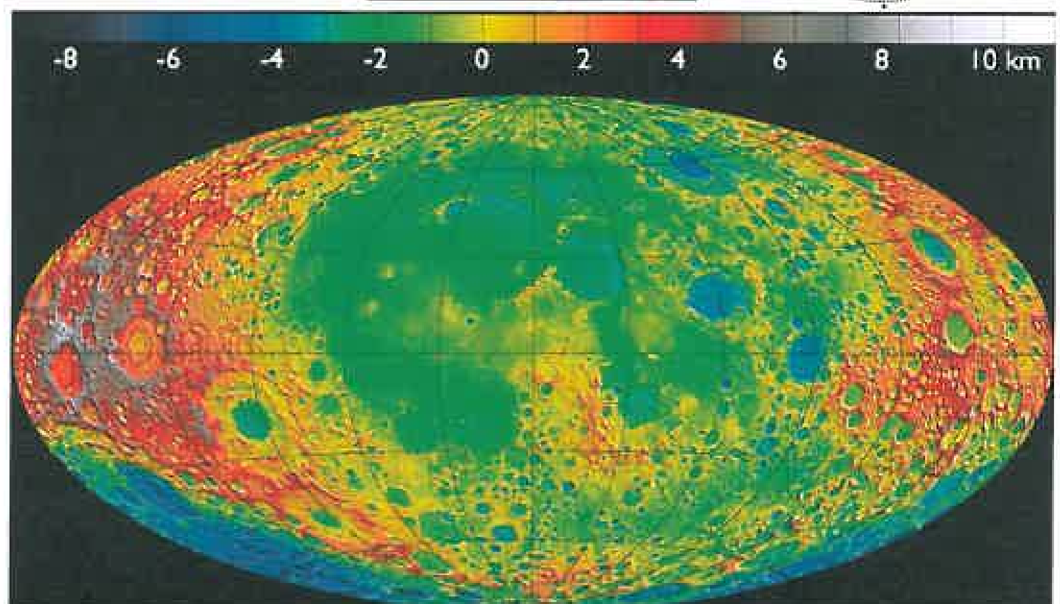

Equal Area projection of lunar topography developed from 1 billion LOLA measurements
Resolution: N/S ~20m; E/W ~0.1 deg (4.5km at equator, 200m at >85 lat)

ICESat-2 ATLAS Instrument

Multi-beam Micropulse Laser Altimeter

- Single laser beam split into 6 beams
- 10 m ground footprints
- 10 kHz rep. rate laser (~1mJ)
- Multiple detector pixels per spot
- On-board boresight alignment system
- Laser Reference System gives absolute laser pointing knowledge

Ground Track and Footprint

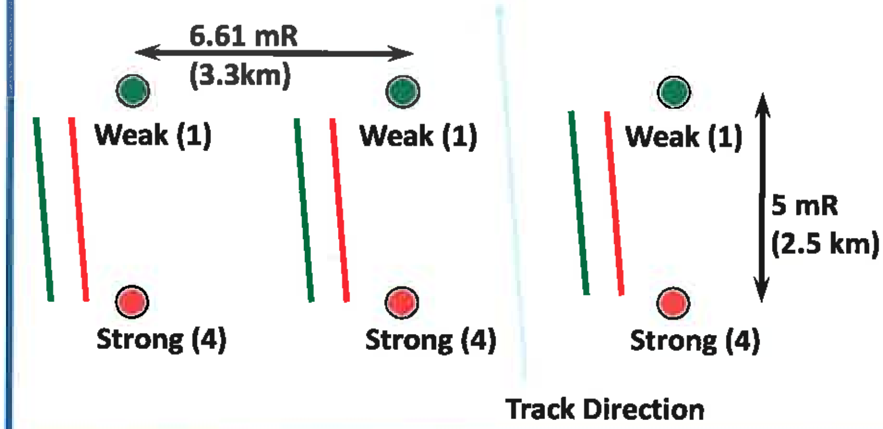

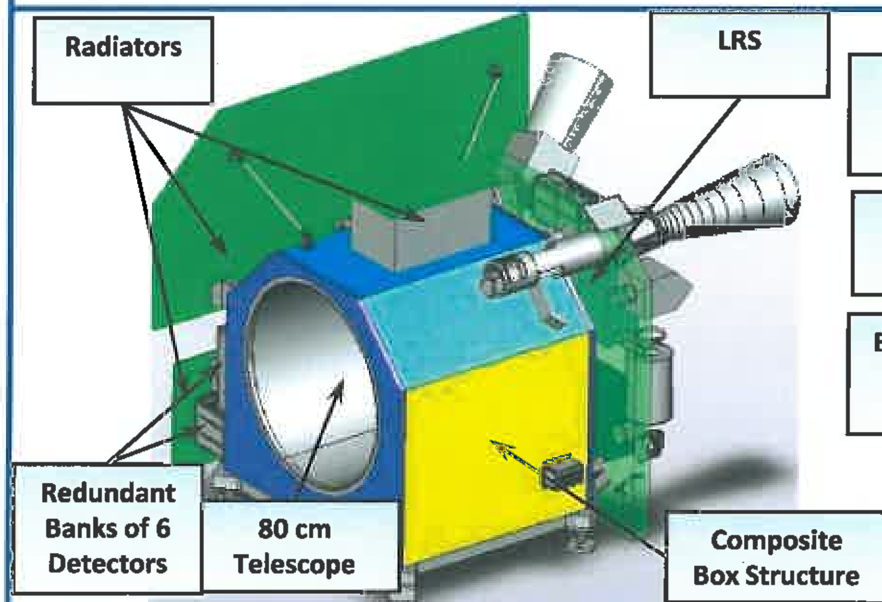

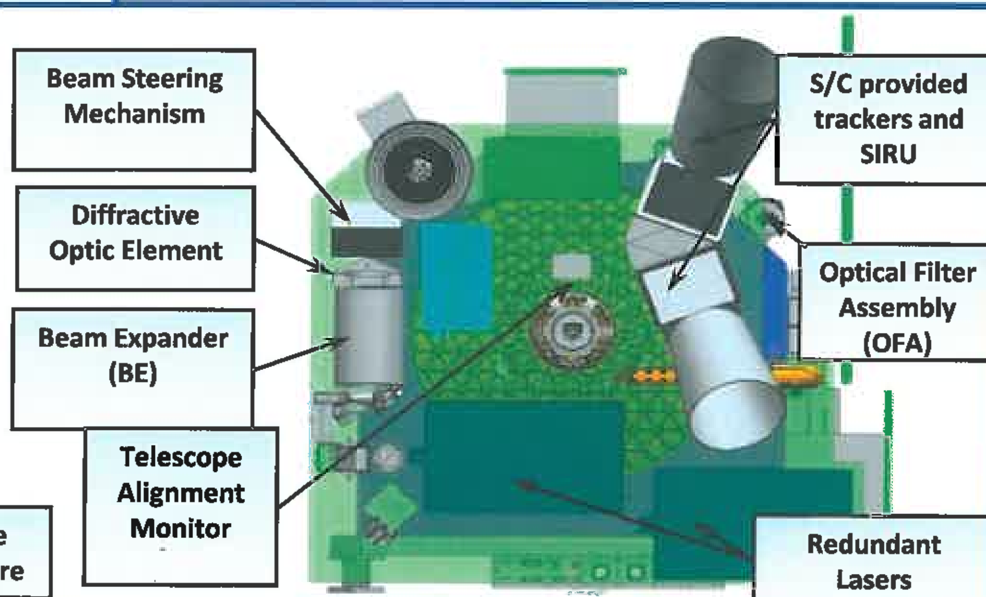

ICESat-2 Flight Lasers

- Significant increase in laser technology compared to previous space missions
  - High repetition rate
  - High power
  - Short pulse width
  - 10^{12} shot lifetime

- Frequency doubled Master Oscillator/Power amplifier architecture
  - > 1 mJ of 532 nm output at 10 kHz.

- Qualification laser is currently in EMI testing and is scheduled to complete testing in by Oct.

- Flight lasers are on track for delivery in late 2014.

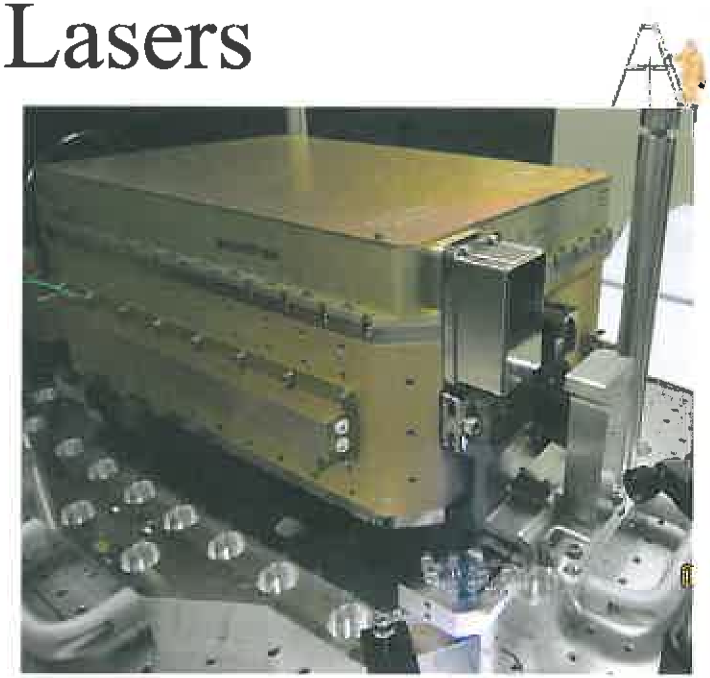

Global Ecosystem Dynamics Investigation (GEDI)

Instrument and Mission Requirements For Carbon Estimation

GEDI Lidar, Class C Mission

International Space Station (ISS)

- Platform provides coverage of nearly all tropical and temperate forests

Self-contained Laser Altimeter

- 3 lasers produce 14 ground tracks
- Precise ranging, attitude and position sensors

Active Pointing Control System

- Provides pointing isolation and enables complete coverage of 500 m grid cells

Requirements		
• 25 m footprints • canopy profile accurate to 1 m • geolocation < 10 m for plot calibration	• 14 beams w/ active pointing to ensure sufficient tracks through cell • 60 m posting for sufficient samples along track	• 500 m grid spacing to capture disturbance impact • Biomass error < 20% at pixel level to accurately estimate emissions and constrain large-area carbon estimates

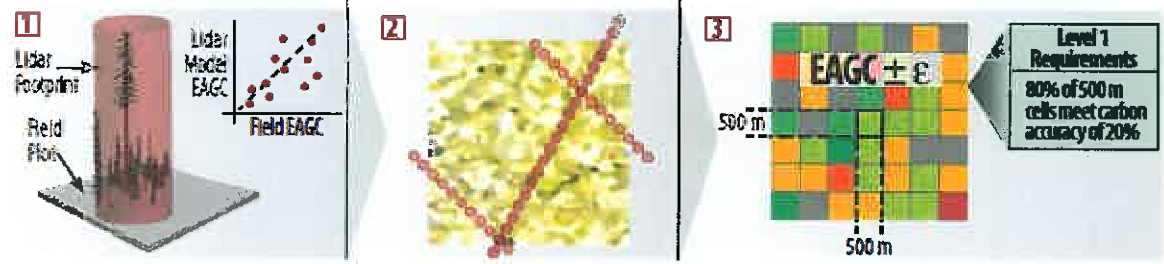

Payload

The waveform lidar technique utilized by GEDI Lidar is the only remote sensing technique that has demonstrated the ability to provide 3-D canopy profile information at the required resolution and accuracy across the full range of canopy cover and environmental conditions.

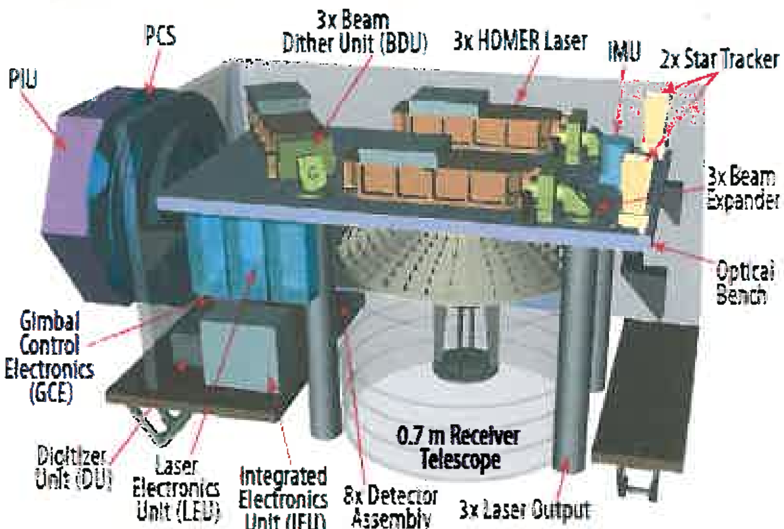

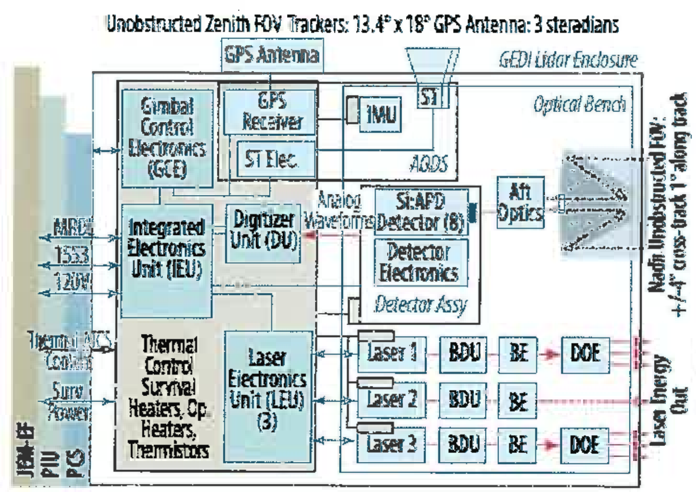

Multi-beam Lidar Coverage

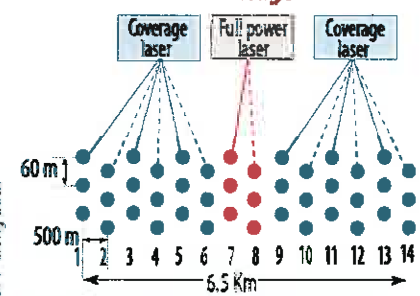

GEDI's 3 lasers generate a balanced complement of 14 ground tracks that achieve the coverage and canopy penetration required to accurately assess biomass in temperate and tropical forests.

Mission Characteristics

Launch Vehicle: Space-X Falcon 9/Dragon

Platform: ISS JEM-EF, Orbit: 410 km (avg), 51.6°

Mass: 230 kg; ISS capability 500 kg; Margin 117%

Volume: 1.7 m X 0.8 m X 0.8 m

Power: 516 W; ISS capability 1500 W; Margin 190%

Data rate: 2.1 Mbps; ISS capability 5 Mbps; Margin 138%

JEM-EF on ISS, equatorial-to-mid-latitude orbit

High Output Maximum Efficiency Resonator

- The HOMER Laser - A highly efficient, TRL6, solid-state laser transmitter for altimetry and lidar.
- Several copies have been produced for TRL advancement. Current systems still operational:
  - HOMER-1 - TRL5 sealed unit for lifetest and flight-like components
  - HOMER-2 - TRL6, flight-like processes, environmental and life testing
  - HOMER ETU - **flight ready design for ISS**, ready for fabrication
- HOMER Development Goals from 2001 to present:
  - ✔ Reduce part count (2/3 reduction from similar systems)
  - ✔ Achieve highest reported efficiency.
  - ✔ Demonstrate > 10B shots (5X – 10X other systems)
  - ✔ Simplify design for reliable assembly.
  - ✔ Demonstrate unmatched lifetime.
  - ✔ Demonstrate unmatched decay rate.
  - ✔ Employ no Beryllium.
  - ✔ Survive GEVS vibration and TVAC.

Output power	13 mJ (1064 nm) in far field central lobe (@ 15 mJ near field)
Wavelength	1064.3 nm +/- 0.2 nm
Pulse width	10 ns +/- 2 ns (FWHM)
Pulse Repetition Freq.	241 Hz
ΔTemp range (Operating)	±2°C (recorded at the LDA pedestal base)
Spatial Mode	Single Gaussian spatial mode, radially symmetric (TEM00)
Temporal Mode	Gaussian with trailing edge pulse porch ≤ 2% of pulse peak amplitude
Divergence (after BX)	57.5 mrad +/- 5 mrad (374 km altitude)
Pointing Jitter	Shot to shot jitter (1 sigma) < 5 mrad
Lifetime per Laser	> 8 Billion Shot @ 35% Duty Cycle over 3 yr Mission (minimum)

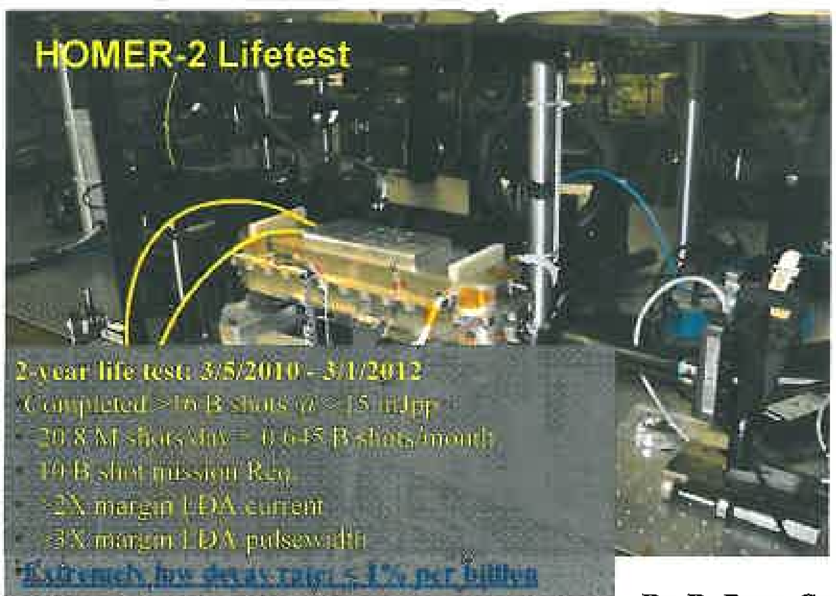

HOMER Flight Transmitter

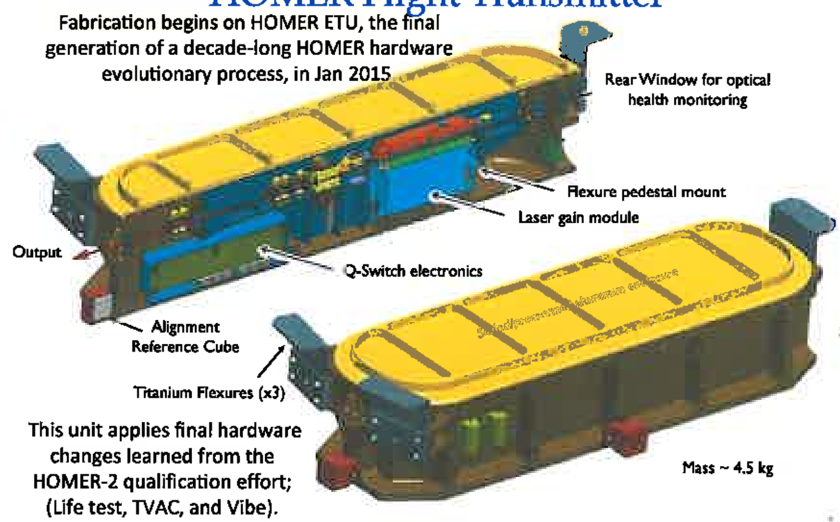

Dr. D. Barry Coyle & Paul R. Stysley / GSFC – Code 554
barry.coyle@nasa.gov; paul.r.stysley@nasa.gov

GRACE follow-on (Gravity Recovery And Climate Experiment)

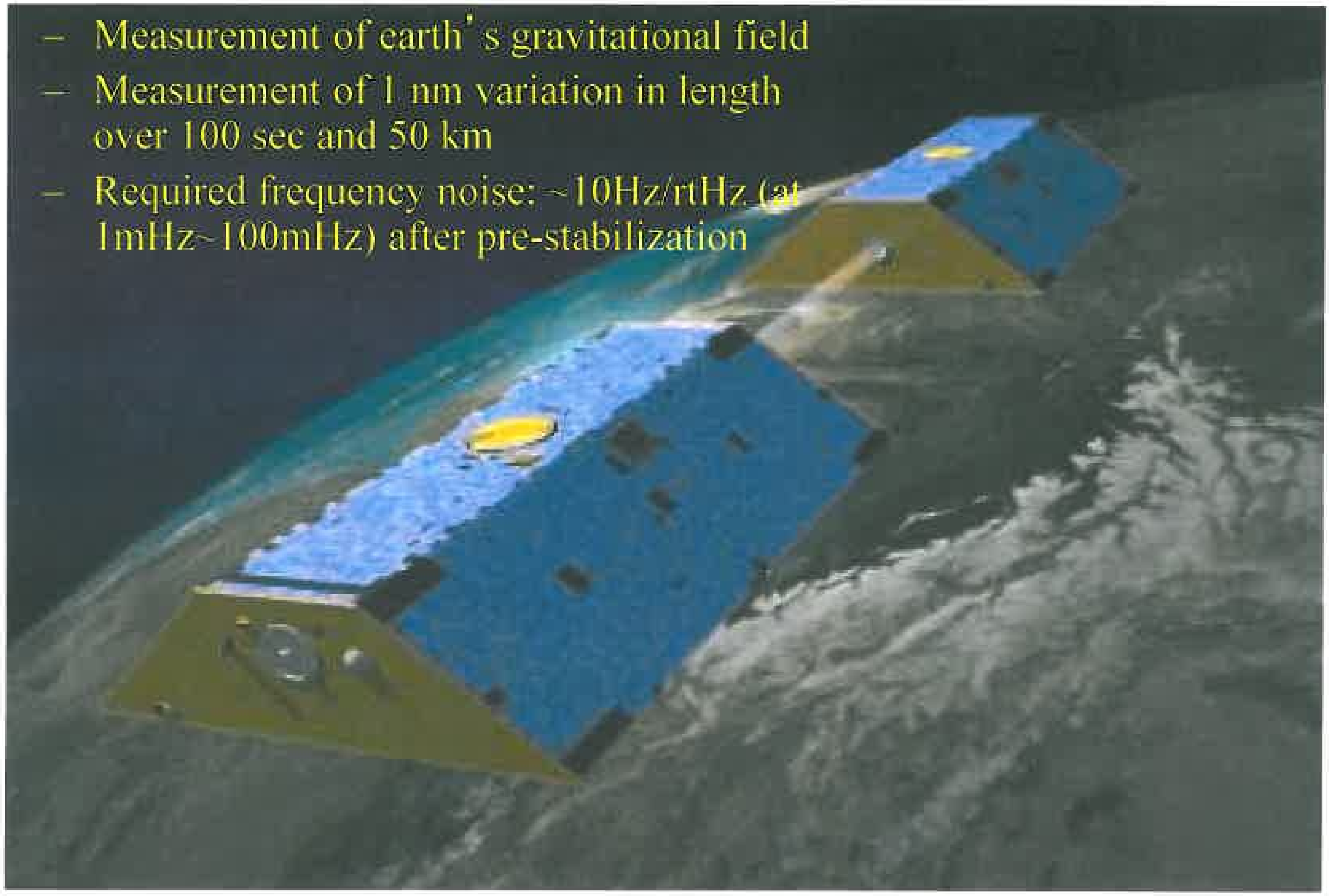

- Measurement of earth's gravitational field
- Measurement of 1 nm variation in length over 100 sec and 50 km
- Required frequency noise: ~10Hz/rtHz (at 1mHz~100mHz) after pre-stabilization

GRACE-FO Laser (Baseline)

- Non-planar ring oscillator (NPRO) Nd:YAG laser provides tunability for locking to cavity
  - Laser wavelength adjusted by changing dimensions of YAG crystal using PZT glued to crystal and thermal adjustment
- Space-qualified NPRO laser available from Tesat Spacecom

NPRO laser head

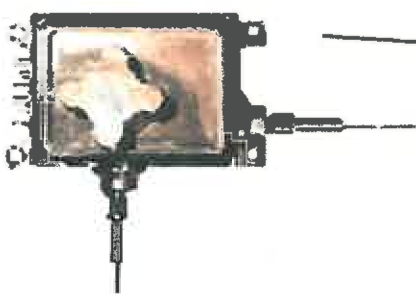

Laser pump diode assembly

Lunar Laser Communications Demonstration (LLCD)

- NASA's first high rate (625 Mbps downlink - 20 Mbps uplink) space laser communications demonstration
- Space terminal integrated on the Lunar Atmosphere and Dust Environment Explorer (LADEE)
- Launched on 6 September 2013 from Wallops Island on Minotaur V
  - Completed 1 month transfer
  - 1 month lasercomm demo @ 400,000 km
    - 250 km lunar orbit
  - 3 months science
    - 50 km orbit
    - 3 science Payloads
      - Neutral Mass Spectrometer
      - UV Spectrometer
      - Lunar Dust Experiment

LLCD diode oscillator/fiber amplifier MOPA laser transmitter
(built by MIT-LL)

Laser Communication Relay Demonstration

LCRD Payload and Host Spacecraft

LCRD Flight Payload
2 Optical Relay Terminals
- **10.8 cm aperture**
- **0.5 W transmitter**

Space Switching Unit

1244 Mbps DPSK
311 Mbps 16-PPM

1244 Mbps DPSK
311 Mbps 16-PPM

Table Mountain, CA

LCRD Ground Station 1
1 m transmit and receive aperture
- **20 W transmitter**

White Sands, NM

LCRD Ground Station 2
15 cm transmit aperture
- **20 W transmitter**

40 cm receive aperture

Mission Concept

- Orbit: Geosynchronous
  - Longitude TBD between 162°W to 63°W
- 2 years mission operations
- 2 operational GEO Optical Relay Terminals
- 2 operational Optical Earth Terminals
- Optical relay services provided
  - Ability to support a LEO User
- Hosted Payload
- Launch Date: Dec 2017

NASA Space Laser Technology
AGENDA

I. Overview of existing and near-term space laser systems

II. Monolithic solid state lasers

I. Future missions

ATLAS laser – is there a “better” way?

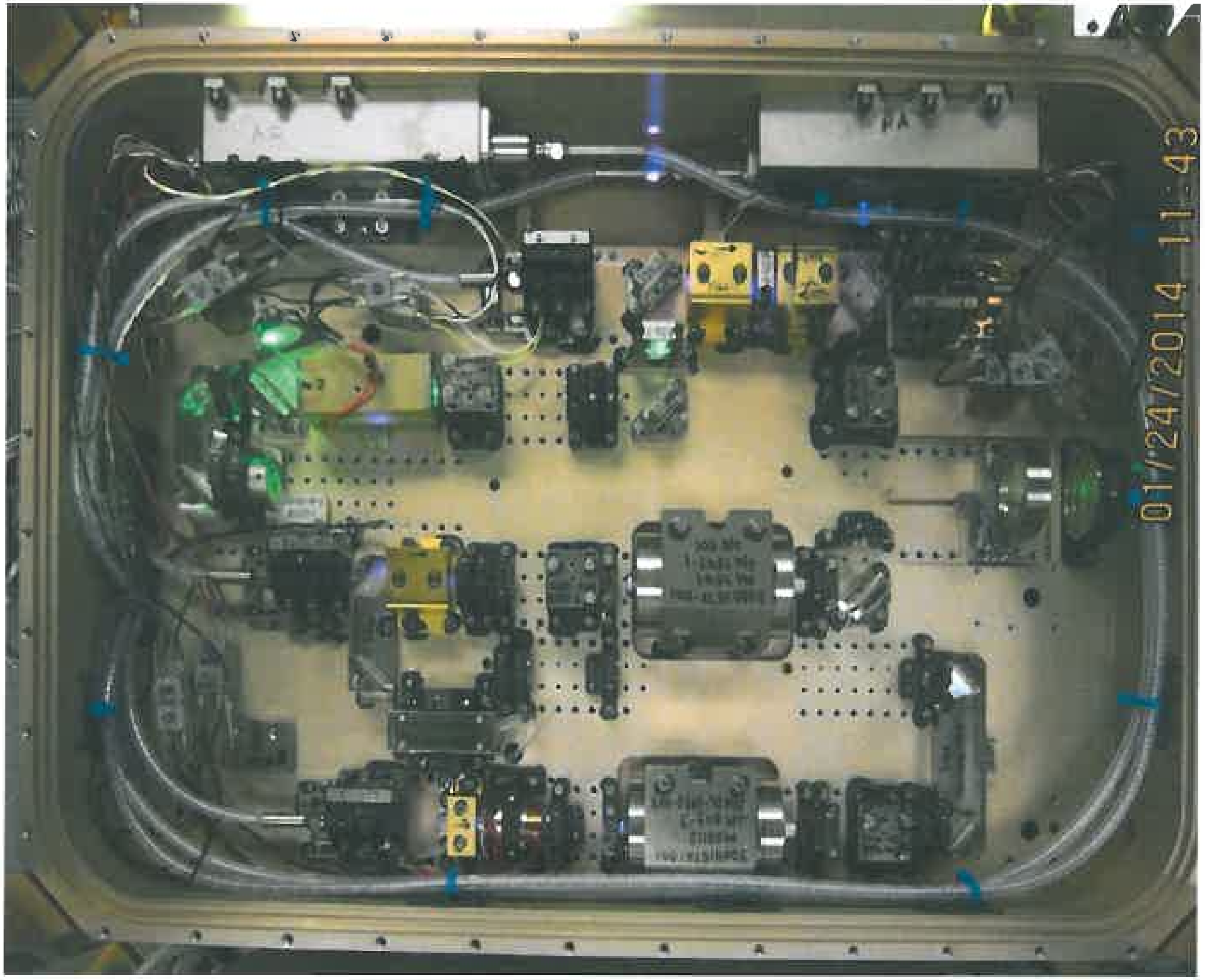

Monolithic Lasers in Use Today

Semiconductor Lasers

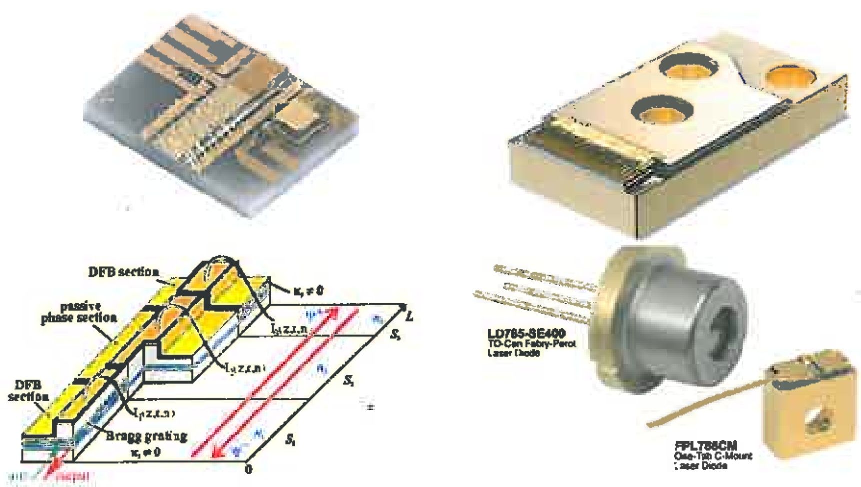

Fiber Lasers

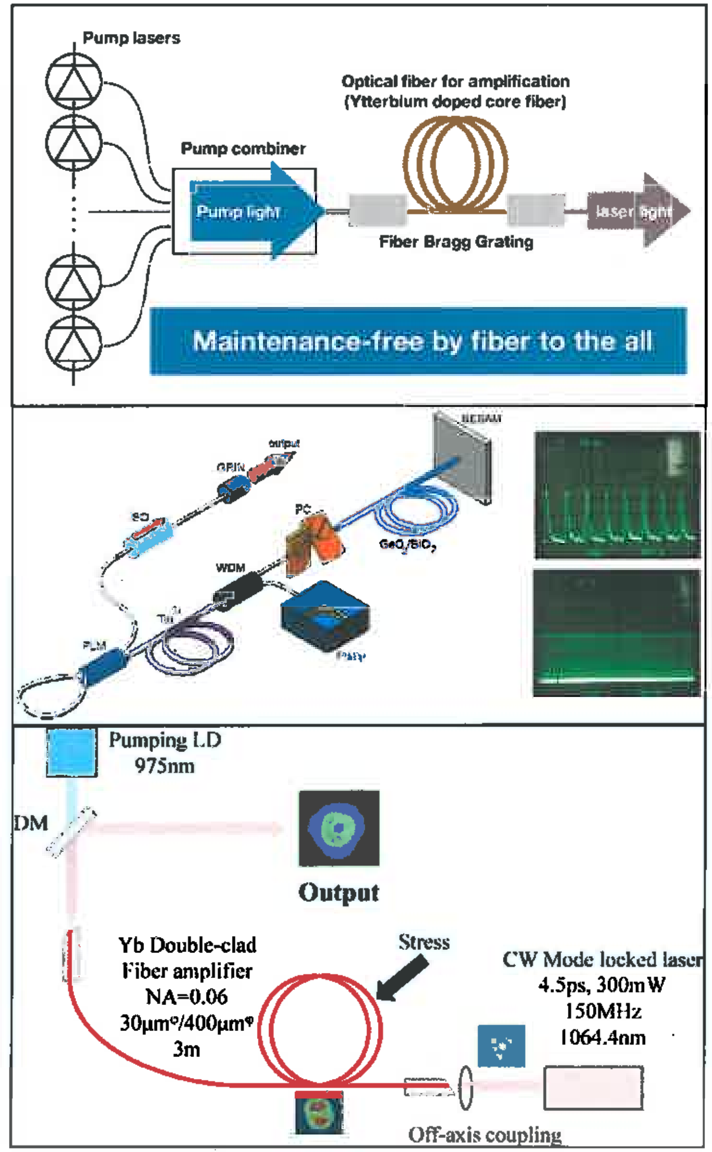

Microchip (Solid State) laser

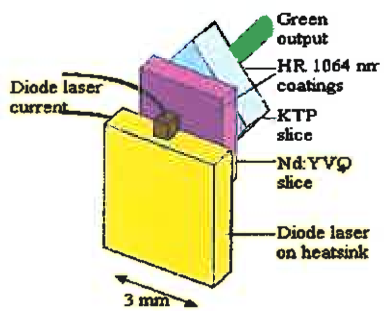

Non-Planar Ring Oscillator (NPRO)
(T. Kane, R. Byer – Stanford U. -1984)

nd inertial rotation sensing.
Ideally, a continuous-wave homogeneously broadened ıser should oscillate in a single axial mode. The laser ·ansitions in Nd:YAG are primarily phonon broadened, › the assumption of homogeneity is met. However, ·hen a Nd:YAG laser is contructed with a standing- ·ave linear resonator, the threshold of the second axial ıode is near that of the first. At the nulls of the ;anding wave created by the initial axial mode, stim- lated emission does not take place, and the gain is not ıturated. This spatially modulated gain, termed ›atial hole burning, allows other axial modes to reach ıreshold and oscillate.[2]
A unidirectional ring resonator has no standing wave, ıd therefore spatial hole burning is eliminated. Much igher single-mode power is available from a ring than ·om a linear resonator even without the addition of ·lective loss elements, such as étalons. Successful igh-power, single-mode operation of uni ngs has been achieved with arc-lamp-pu

and totally internally reflecting.
Most ring lasers use a resonator that is entirely within a plane. There are sometimes advantages to a non- planar geometry that are worth the greater complexity. Dorschne at Raytheon has described a nonplanar he- lium–neon ring laser that, when used as a gyroscope, overcomes the problem of self-locking or lock-in.[7] Researchers in the Soviet Union have built nonplanar Nd:YAG ring lasers and have studied the mode struc- ture, temporal dynamics, and polarization of these la- sers.[8] Biraben[9] suggested that single-mode dye lasers

February 1985 / Vol. 10, No. 2 / OPTICS LETTERS 65

ıgle-mode Nd:YAG ring laser

ıd Robert L. Byer
versity, Stanford, California 94305

ccepted November 26, 1984

ıtor contained entirely within a Nd:YAG crystal. When ıal oscillation was obtained with a pump-limited, single-

unidirectional laser is to include a polarizer, a Faraday rotator, and a nonmagnetic polarization rotator, such

1020 OPTICS LETTERS / Vol. 20, No. 9 / May 1, 1995

Single-frequency Q-switched ring laser with an antiresonant Fabry–Perot saturable absorber

B. Braun and U. Keller
Ultrafast Laser Physics, Institute of Quantum Electronics, Swiss Federal Institute of Technology, ETH Hönggerberg-HPT, CH-8093 Zürich, Switzerland

Received January 3, 1995

We passively Q switched a monolithic Nd:YAG ring laser [monolithic isolated single-mode end-pumped ring laser (MISER)] using an evanescent-wave coupled antiresonant Fabry–Perot saturable absorber. Single-frequency, 0.7-μJ pulses with a pulse width below 100 ns at an ~1-MHz repetition rate are demonstrated. Pulse width and repetition rate can be varied by changing the distance and thus the coupling strength between the crystal and the absorber.

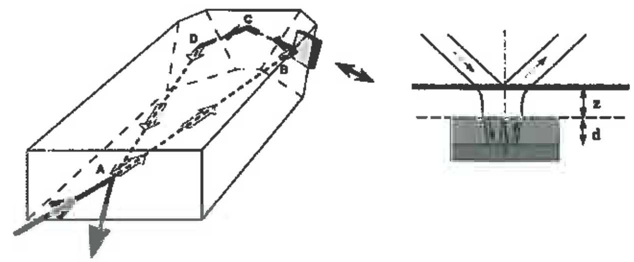

Fig. 1. Layout of the MISER with an A-FPSA coupled to a total-internal-reflection point and (at the right) a schematic of the interface between the MISER and the A-FPSA.

Continuous-Wave (CW) Single-Frequency IR Laser
NPRO® 125/126 Series

JDSU

Key Features
- 1319 or 1064 nm outputs available
- Fiber-coupled output
- Proven nonplanar ring oscillator (NPRO) design
- Superior power stability
- Narrow linewidth
- Tunability
- Ease of use
- Ideal for OEM applications

COHERENT.

Features
- Non-planar ring oscillator (NPRO) technology for ultra-stable operations
- Diffusion bonded, quasi monolithic cavity for ultra-stable emission
- Q-switched operation with Cr^{4+}:YAG saturable absorber crystal
- Low noise control electronics
- User-installed, turn-key operation

250 mW, 50 μJ at 5 kHz

Power scaling NPRO with disk laser

July 15, 2004 / Vol. 29, No. 14 / OPTICS LETTERS 1635

1.6 W of single-mode output power from a novel power-scaling scheme for monolithic nonplanar ring lasers

Hagen Zimer and Ulrich Wittrock

Photonics Laboratory, University of Applied Sciences Münster, Stegerwaldstrasse 39, 48565 Steinfurt, Germany

Received January 13, 2004

A novel monolithic ring laser with high potential for power scaling, the disk nonplanar ring oscillator, is presented. We achieved power scaling by reducing the pump-light-induced aberrations. The basic idea of our approach is to attach a thin Nd:YAG disk to an undoped nonplanar YAG ring resonator while the other side of the disk is mounted on a heat sink. First promising experiments have demonstrated a single-frequency cw output power of 1.6 W at 1.06 μm with a slope efficiency of 45%. Power scaling to several watts seems to be possible. © 2004 Optical Society of America

OCIS codes: 140.3570, 140.3480, 140.3560, 140.3410, 140.3580, 140.3530.

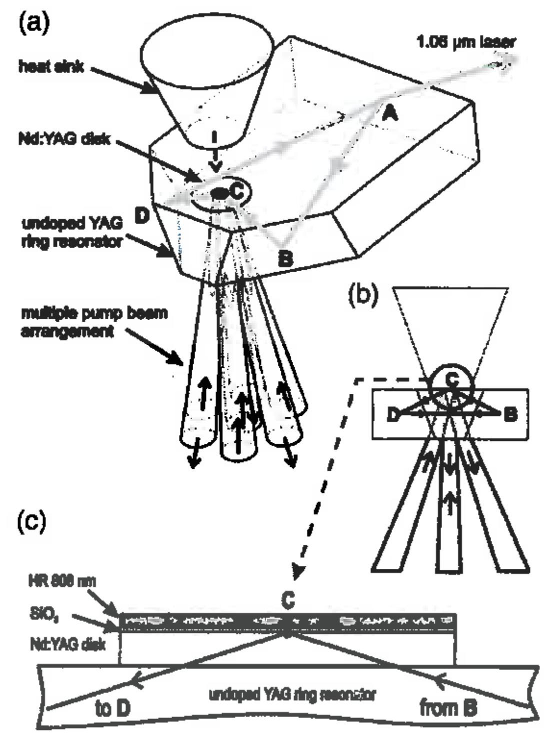

Fig. 1. (a) Nd:YAG disk NPRO, (b) front view into the *BCD* plane, (c) enlarged section of the disk about TIR point C.

Monolithic laser advantages

Parameters	Single element monolithic laser and multi-element laser array
Spectral	DFB/DBR helps with spectral narrowing, spectral stability and single frequency operation.
Spatial	Thermal lens and passive q-switching provides soft aperturing to ensure high beam quality
Temporal	Short cavity means short optical pulses
Energy/Power	Design to produce 50 μJ; also per design to produce 8.4 kHz - average power ~0.42W
Repetition Rate	Pump power driven, also affected by Yb concentration, need iterative processes to optimize concentration for gain and rep rate
Passive QS	Discrete SA element or co-dope with Yb in PTR, no high voltages as in Active QS
Coatings	Bragg mirrors serve as high reflector and output coupler, no coating except for AR to minimize Fresnel reflection for pump and lasing wavelength, avoid the issue of optical damage to coating.
Nonlinear Effects	No detrimental nonlinear effects
Reliability	Use highly fiber coupled pump lasers used in telecom industry. Multiple lasers mean losing one laser can still do majority of science - built in redundancy.
Pump configuration	Fiber coupled pumps for compact and robust design. Using microlens array for coupling pump light into laser array.
Laser Cavity	Closed cavity immunes to contamination inside laser cavity, which usually has the highest fluence. Monolithic design to minimize number of components.
Pointing Stability	End gratings formed the lasing axis, thermal lensing and soft aperturing from PQS provides additional pointing stability
Alignment Sensitivity	Monolithic design means robustness. No to low misalignment concerns with laser resonator.
Thermal Control	Will examine the use of embedding loop heat pipes (LHP) or microchannel cooler(MCC) into the laser array for efficient thermal management. LHP has been used successfully in spaceflight lasers and MCC has been used extensively in packaging of high power semiconductor laser arrays

Solid state monolithic laser with Volume Bragg Grating mirrors

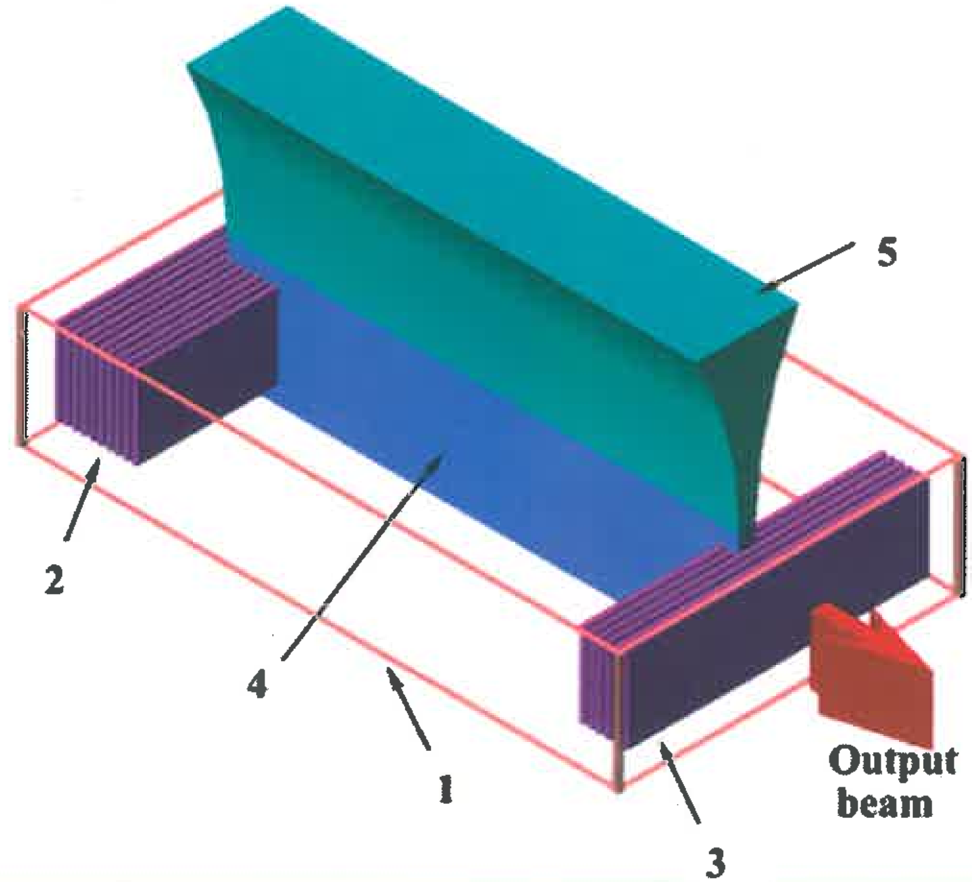

Possible geometry of a monolithic solid state laser in PTR glass doped with rare earth ions. 1 - rear-earth doped PTR-glass wafer; 2 – high efficiency VBG as a feedback coupler; 3 – low efficiency VBG as an output coupler; 4 - pumped volume in active PTR-medium; 5 - pumping beam from LD bars.

Monolithic Yb:glass CW solid state laser

2156 OPTICS LETTERS / Vol. 39, No. 7 / April 1, 2014

DBR and DFB lasers in neodymium- and ytterbium-doped photothermorefractive glasses

A. Ryasnyanskiy,[1,*] N. Vorobiev,[2] V. Smirnov,[1] J. Lumeau,[2,3] L. Glebova,[1] O. Mokhun,[1] Ch. Spiegelberg,[1] Michael Krainak,[4] A. Glebov,[1] and L. Glebov[2]

[1]OptiGrate Corp, 562 South Econ Circle, Oviedo, Florida 32765, USA

[2]CREOL—The College of Optics and Photonics, University of Central Florida, Orlando, Florida 32816-2700, USA

[3]Aix-Marseille Université, CNRS, Centrale Marseille, Institut Fresnel, UMR 7249, Marseille 13013, France

[4]NASA Goddard Space Flight Center, 8800 Greenbelt Rd., Greenbelt, Maryland 20771, USA

*Corresponding author: aryasnyanskiy@optigrate.com

Received January 3, 2014; revised March 5, 2014; accepted March 10, 2014; posted March 11, 2014 (Doc. ID 204149); published March 31, 2014

The first demonstration, to the best of our knowledge, of distributed Bragg reflector (DBR) and monolithic distributed feedback (DFB) lasers in photothermorefractive glass doped with rare-earth ions is reported. The lasers were produced by incorporation of the volume Bragg gratings into the laser gain elements. A monolithic single-frequency solid-state laser with a linewidth of 250 kHz and output power of 150 mW at 1066 nm is demonstrated. © 2014 Optical Society of America

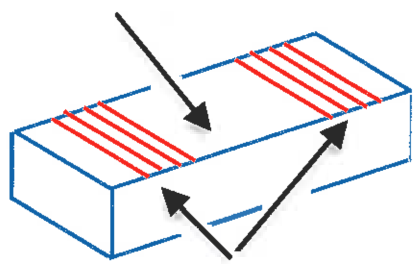

Monolithic Master Oscillator Power Amplifier (MOPA)

Semiconductor Monolithic MOPA

linewidths, together with the shift in the peak of the $^4F_{3/2} \rightarrow {}^4I_{11/2}$ fluorescence to 1051 nm, suggest a glass network structure similar to that previously reported for neodymium pentaphosphate glasses [6]. From the narrow spectrum obtained for erbium-doped fibres, it is likely that a similar glass structure also exists in the Er/Yb co-doped fibres.

The technique is also readily varied to allow the incorporation of a variety of other glass-forming and modifying oxides. Just as phosphoric acid (H_3PO_4), a weak triprotic acid, serves as a source for phosphorus pentoxide (P_2O_5) similarly boric, stannic, arsenic, selenic, silicic and germanic acids may serve as a source of boron, tin, arsenic, selenium, silicon and germanium oxides, respectively.

Conclusions: A technique for controllably fabricating fibres

High-power diffraction-limited semiconductor sources have been sought after for a number of years. Semiconductor lasers have demonstrated operation to high output powers, in excess of 120 W CW from a single monolithic chip [1]; however, coherent operation of semiconductor lasers has been limited to significantly lower output powers. Several monolithic approaches have been studied with the goal of demonstrating coherent output powers in excess of 1 W CW including anti-guide laser arrays [2–4], monolithically integrated active

Solid-state (crystal/glass) MONOLITHIC MOPA

?

Yb:YAG Microchip Laser with Passive Q switch (Raytheon)

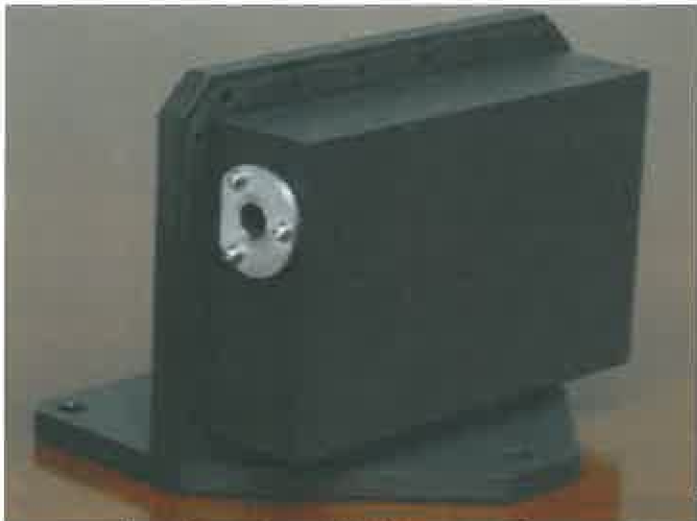

Laser Output Beam Parameters

Pulse Energy:	0.1 mJ
Repetition Rate:	10 kHz
Wavelength:	1030.2 nm
Linewidth:	17 pm
Polarization Ext:	25 dB
Pulsewidth:	0.83 nsec
Beam Quality M2:	1.3
O-O Efficiency:	25%

Laser Operating point

Diode Current:	4.5 A
Diode Output Power:	3.9 W
Chiller Temp:	29.8 ^{0}C
Diode Temp:	31 ^{0}C
μChip Temp:	17.8 ^{0}C
VBG Temp:	20 ^{0}C

Raytheon
Space and Airborne Systems

Planar waveguide power amplifier
Solid state MOPA (Raytheon)

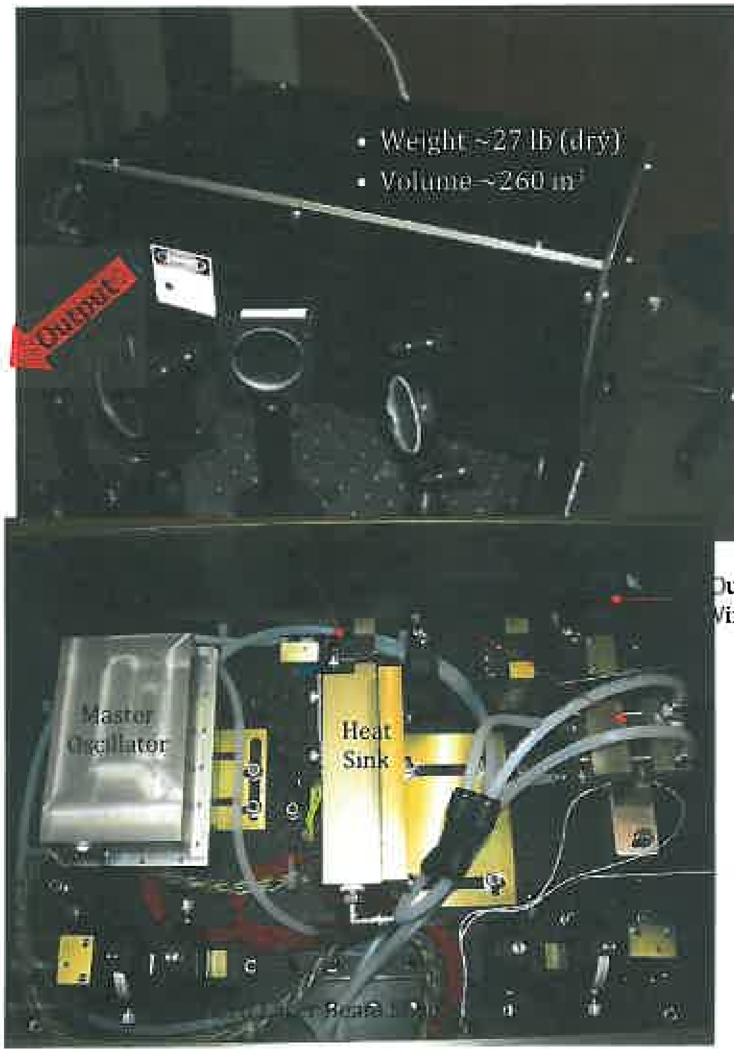

Output Window

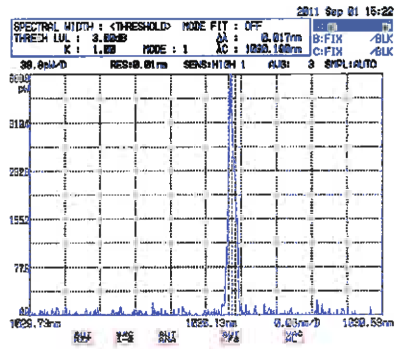

Wavelength ~1030.2 nm;
<20 pm spectral width

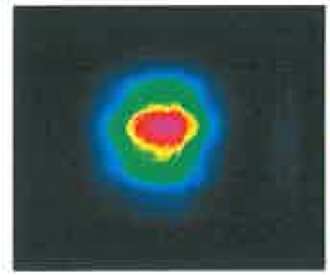

NF Image at ~84 cm from MOPA Output
FW1/e^2 size: 2.6 mm x 3.3 mm

FF Image

MO Nominal Operating Point

Pulse Energy	0.1 mJ
Repetition Rate	10 kHz
Wavelength	1030.2 nm
Linewidth	0.018 nm
Polarization ER	25 dB
Pulsewidth	0.8 nsec
Beam Quality	M^2 ~1.3
Opt-Opt Efficiency	25.6%
El-Opt Efficiency	12.8%

MOPA Nominal Operating Point

Pulse Energy	2.2 mJ
Repetition Rate	10 kHz
Wavelength	1030.2 nm
Linewidth	0.02 nm
Polarization ER	18 dB
Pulsewidth	0.8 nsec
Beam Quality	M^2~1.1
Opt-Opt Efficiency	24%
El-Opt Efficiency	11%

Raytheon
Space and Airborne Systems

Making lasers with a laser

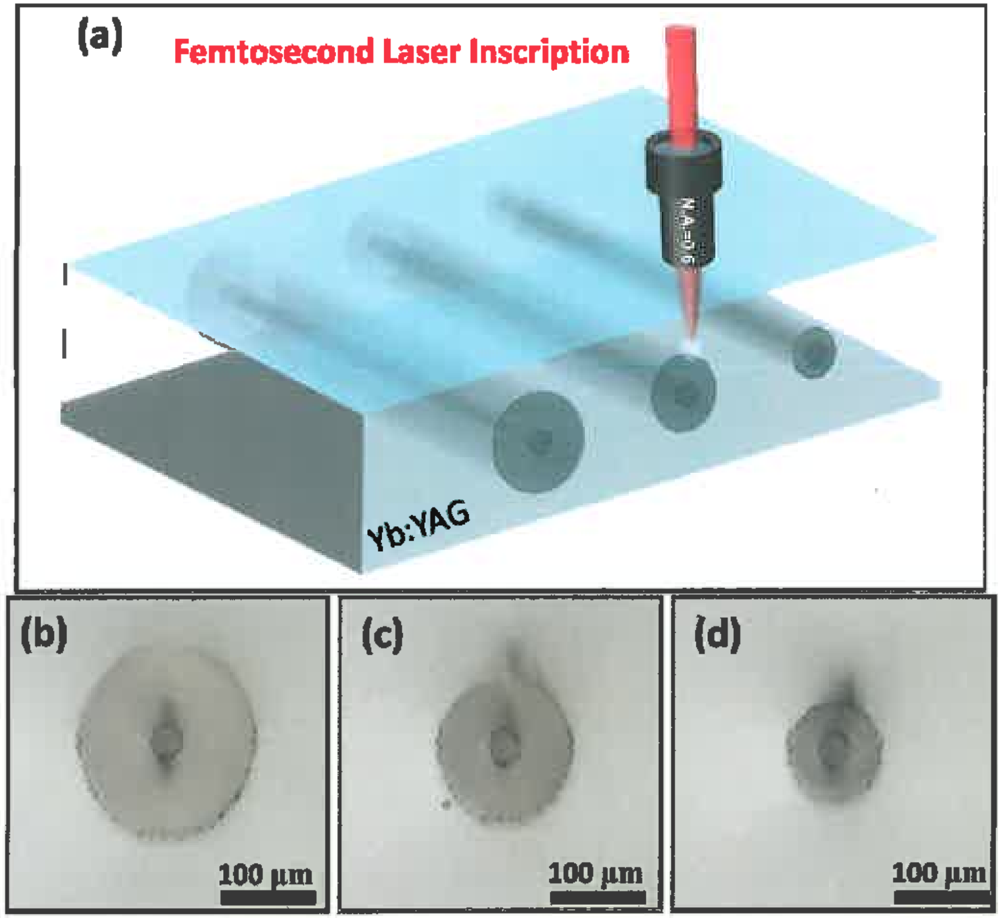

Fig. 1. (a) Schematic of fs-laser inscription process in Yb:YAG ceramics for the double cladding waveguides, and their cross sectional microscope images, which consist of tubular central structures with 30 µm diameter, and concentric larger size tubular claddings with diameters of (b) 200, (c) 150 and (d) 100 µm, respectively.

1 May 2013 | Vol. 3, No. 5 | DOI:10.1364/OME.3.000645 | OPTICAL MATERIALS EXPRESS 647

Double clad monolithic laser Performance

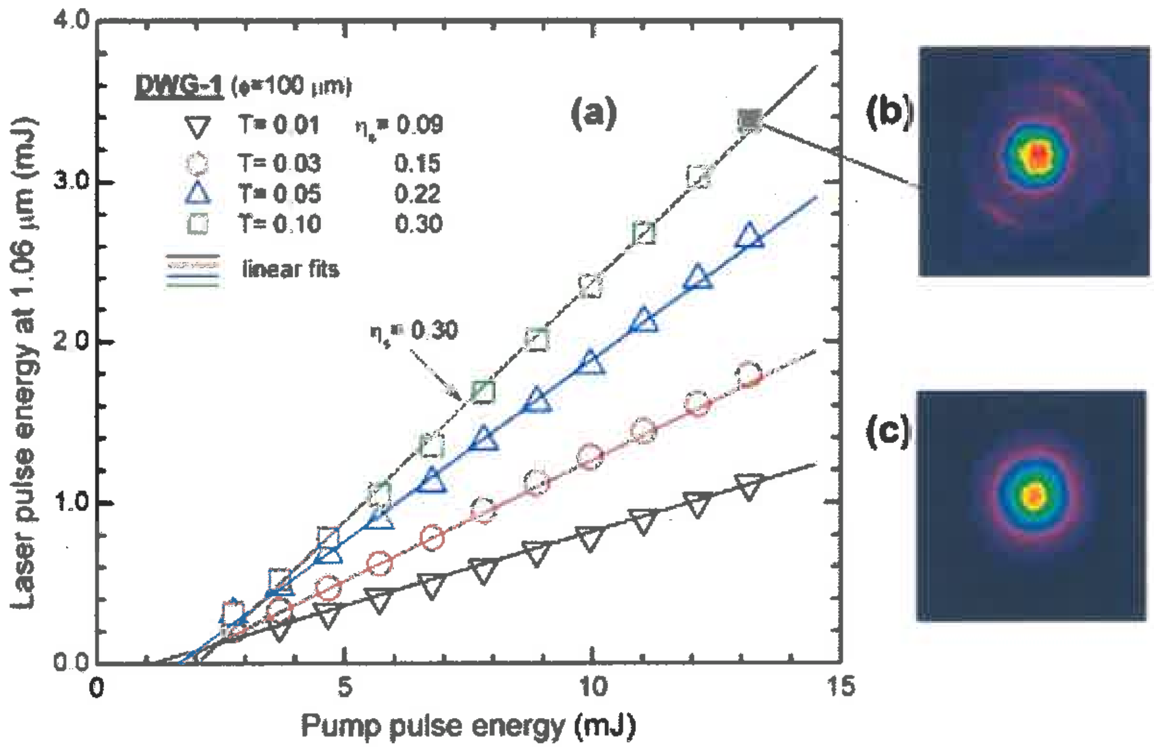

Fig. 4. (a) Laser pulse energy at 1.06 μm versus energy of the pump pulse incident on the DWG-1 waveguide. The near-field distributions are shown at the maximum laser pulse energy (OCM with T = 0.10) for emission in (b) DWG-1 (E_p = 3.4 mJ) and (c) bulk Nd:YAG (E_p = 5.5 mJ).

1 April 2014 | Vol. 4, No. 4 | DOI:10.1364/OME.4.000790 | OPTICAL MATERIALS EXPRESS 794

Optical waveguides in smartphone "Gorilla" glass!

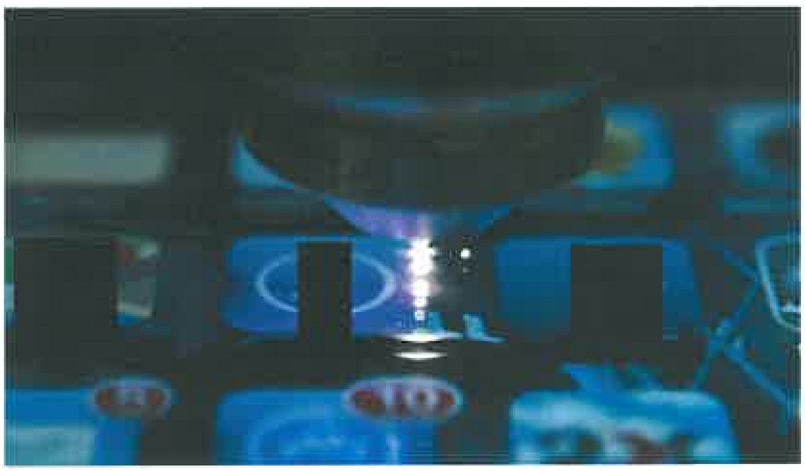

Fig. 1. Laser writing of a photonic device in a smart phone screen. The photograph shows that the waveguide (a horizontal line from the left side) cannot be seen by the naked eye. The white light comes from the plasma generated by the nonlinear absorption of the focused laser.

$$NA \approx \sqrt{n_2^2 - n_1^2} \quad (3)$$

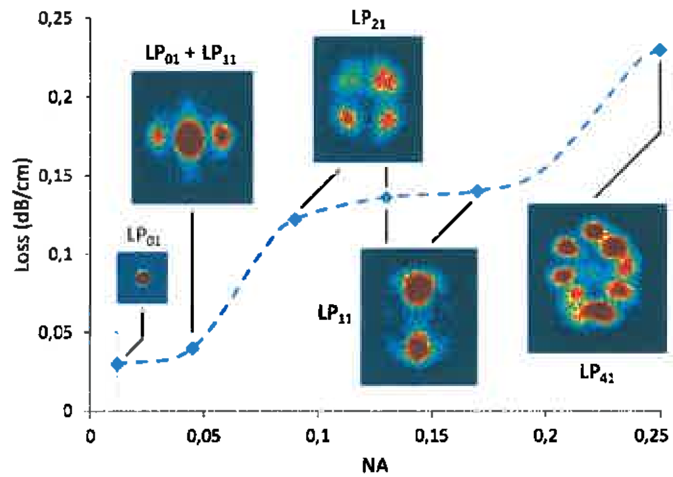

Fig. 7. Loss of the 30 cm multimode waveguide (with a loss of 0.027 dB/cm) with different launch NAs. More modes appear as the NA increases. At an NA of ~0.012, only the LP_{01} mode is seen, and at an NA of 0.25 all modes are seen at the waveguide output by altering the launch conditions.

Graphene waveguide modulator

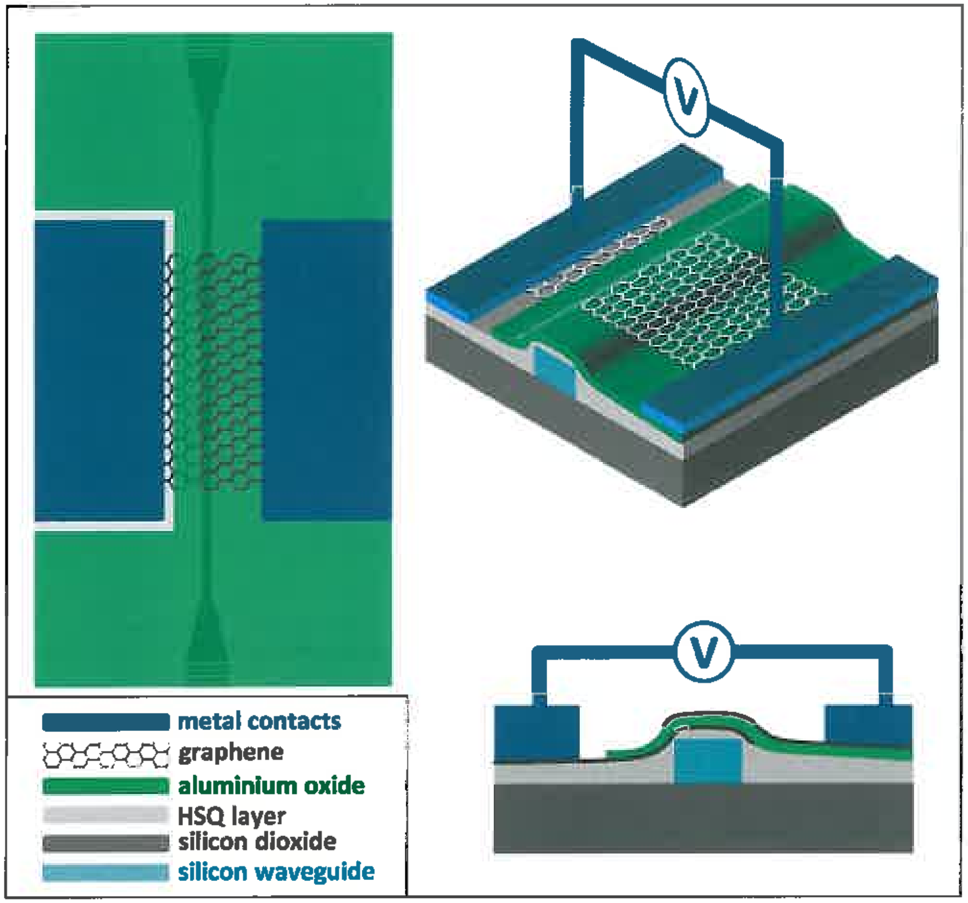

Fig. 1. Top view of device, light was coupled using grating couplers (left). Isometric view of device showing graphene layer on top of Si waveguide (top right). Cross-sectional view of device with graphene layers separated by 94 nm aluminum oxide (bottom right).

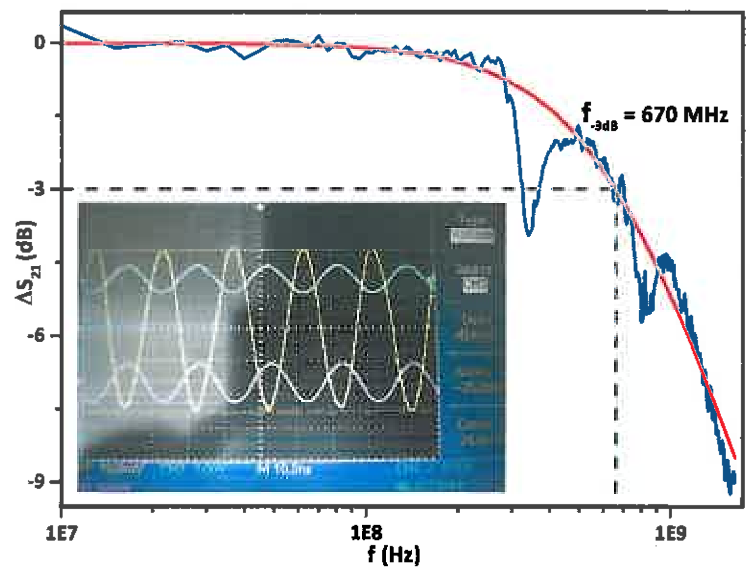

Fig. 3. Relative electro-optical response of the modulator as a function of frequency. f_{-3dB} is 670 MHz. The inset shows the output signal of the modulator at 50 MHz (yellow line) for an AC input voltage V_{PP} = 6 V (purple and cyan lines represent the reference signals).

16 June 2014 | Vol. 22, No. 12 | DOI:10.1364/OE.22.015292 | OPTICS EXPRESS 15297

Q-switched monolithic laser
Passive and active Q-switches

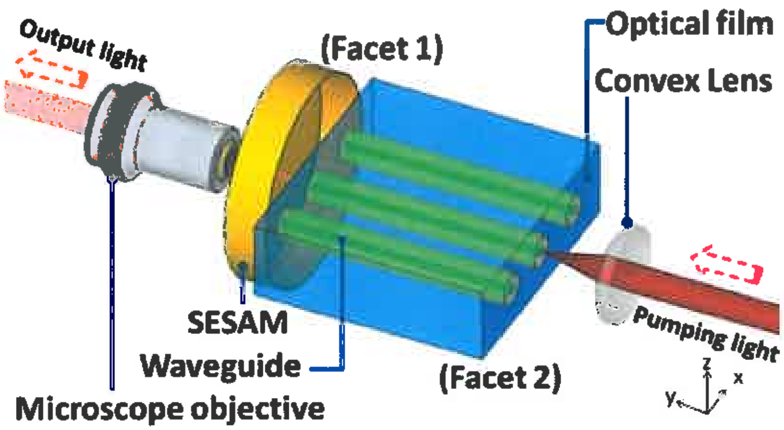

Fig. 2. Schematic plot of the experimental setup for the pulsed laser generation in the double-cladding Nd:YAG ceramic waveguides.

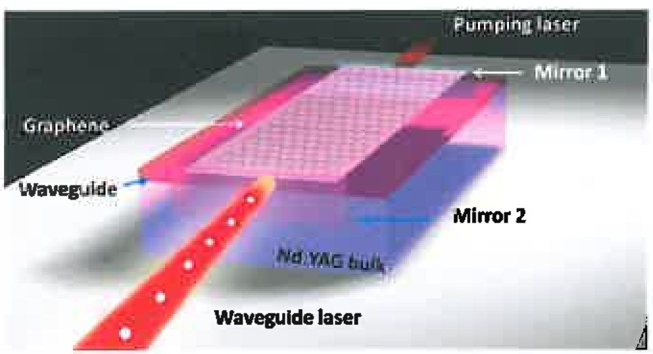

Fig. 1. The experimental scheme for the indirect interaction graphene Q-switched waveguide laser generation.

21 April 2014 | Vol. 22, No. 8 | DOI:10.1364/OE.22.009101 | OPTICS EXPRESS 9101

Planar Waveguide Amplifier for Power Scaling

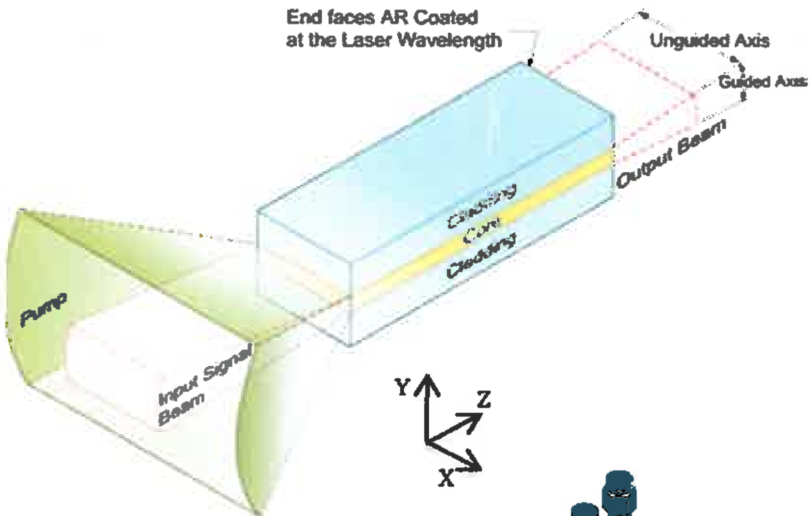

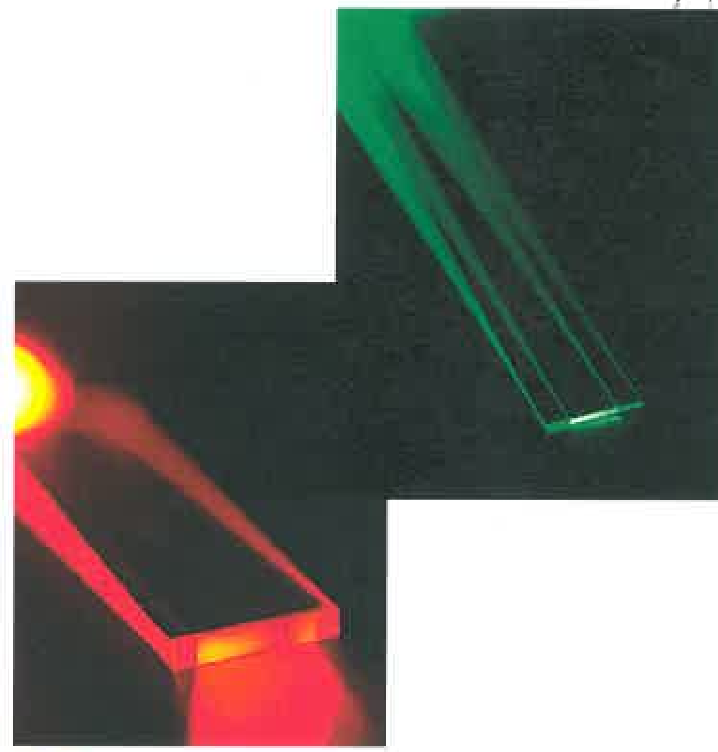

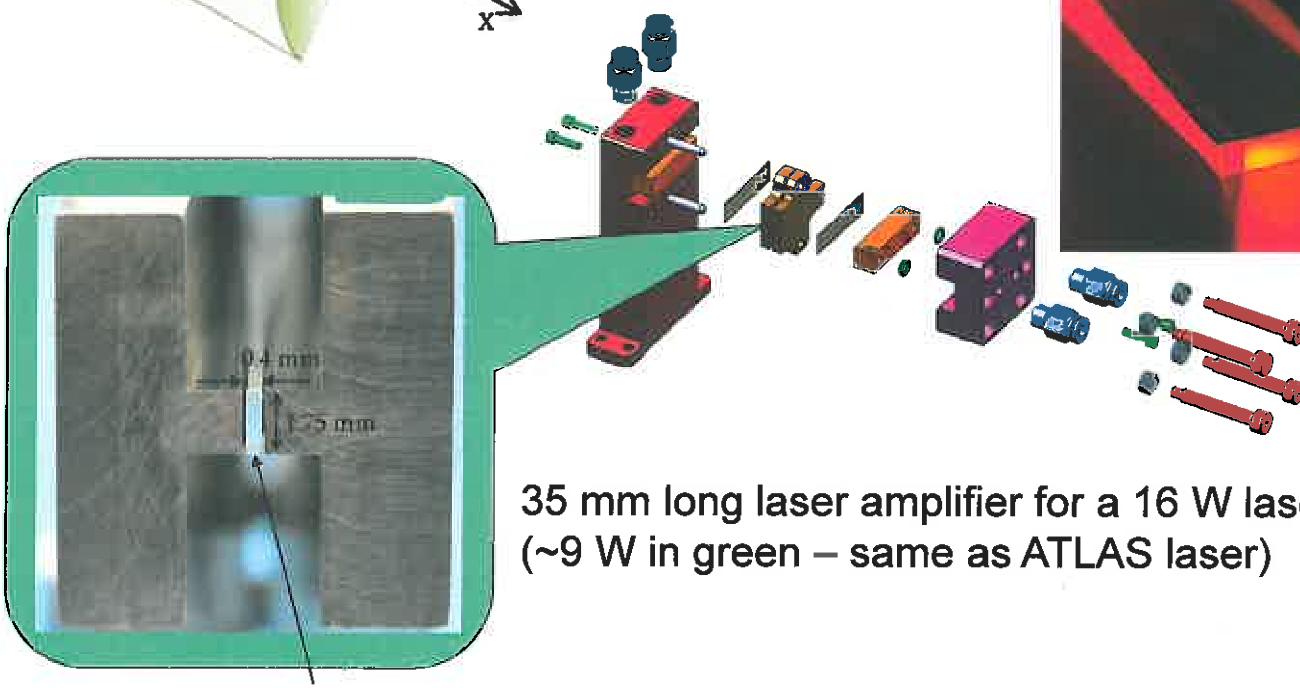

35 mm long laser amplifier for a 16 W laser at IR
(~9 W in green – same as ATLAS laser)

Yb:YAG waveguide core, 40 μm thick, sandwiched by undoped YAG

Optical frequency doubling

1274 OPTICS LETTERS / Vol. 39, No. 5 / March 1, 2014

Highly efficient continuous wave blue second-harmonic generation in fs-laser written periodically poled Rb:KTiOPO$_4$ waveguides

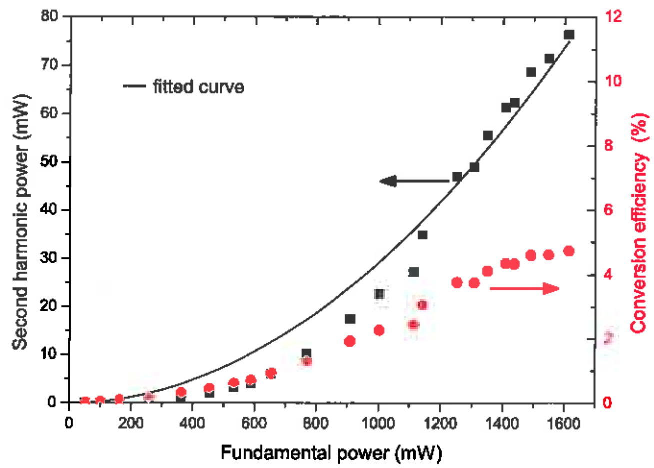

Fig. 1. Second harmonic power (black squares) and conversion efficiency (red dots) versus incident fundamental power at 943.18 nm. Theoretical square-fit of the measured data points (solid line).

NASA Space Laser Technology
AGENDA

I. Overview of existing and near-term space laser systems

II. Monolithic solid state lasers

I. Future missions

"Earth" application – Not just monolithic but monolithic with "compatible" material/process. *Cost driven*

SiN waveguide lasers for CMOS (MIT and UCSB)

3106 OPTICS LETTERS / Vol. 39, No. 11 / June 1, 2014

CMOS-compatible 75 mW erbium-doped distributed feedback laser

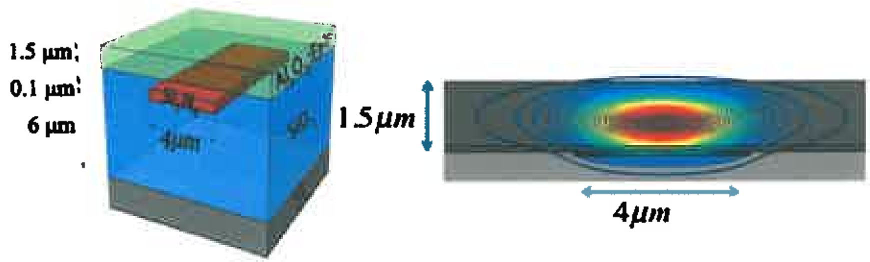

Fig. 1. Waveguides used in this work. (a) Layers used for constructing the waveguide structure within wafer-scale fabrication flow. High-definition masks are used to create waveguides and gratings in the SiN layer, and an erbium-doped glass is deposited as a blanket film. (b) Intensity profile of an inverted ridge waveguide mode with a 4 µm SiN core. The 1563 nm mode is mainly confined in the erbium-doped glass.

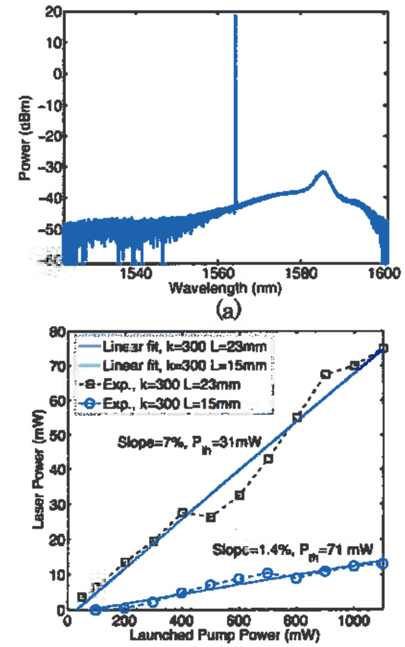

Fig. 2. On-chip DFB laser performance. (a) Single-mode laser emission from the DFB with more than 60 dB suppression of the amplified spontaneous emission (ASE), measured with an OSA with 0.02 nm resolution. The peak around 1588 is due to the Raman-shifted residual pump. (b) Power as a function of launched pump power for two lasers with equal corrugation ($\kappa = 300$), but different grating length ($L = 23$ and 15 mm), lasing at 1563 nm. The cavity with the longer grating shows higher slope efficiency and a lower threshold.

Upcoming approved NASA missions with a space-based laser

Mission	Laser	Launch Date
Cloud-Aerosol, Transport System (CATS) NASA-GSFC	Nd:YVO4 laser (IR, green, UV)	2015
Origins-Spectral Interpretation-Resource Identification-Security-Regolith Explorer. OSIRIS-REx (Lockheed Martin – Advanced Scientific Concepts)	Nd:YAG (IR)	2016
Ice, Cloud & land Elevation SATellite Advanced Topographic Laser Altimeter System (ICESat-2/ATLAS) NASA-GSFC	Nd:YVO4 laser (green)	2017
Gravity Recovery And Climate Experiment-Follow On (GRACE-FO) NASA-JPL	Nd:YAG Monolithic NPRO	2017
Laser Communication Relay Demonstration (LCRD) NASA-GSFC/JPL/MIT-LL	Diode oscillator-erbium fiber amplifier MOPA	2018
Geodynamics of the Earth, Dynamics of Ice (GEDI) NASA-GSFC	Nd:YAG laser (IR)	2019

Upcoming "hopeful" NASA missions with a space-based laser (start before 2024)

Mission	Laser
Jupiter Europa topography	Nd:YAG MOPA (similar to Mercury Laser Altimeter)
Laser communication terminal International Space Station (to LCRD)	Diode oscillator-erbium fiber amplifier MOPA
Deep-space Optical Terminal (JPL)	Diode oscillator-erbium fiber amplifier MOPA
Robotic Servicing	Nd:YAG or Diode oscillator-erbium fiber amplifier MOPA
Earth atmospheric carbon dioxide	Diode oscillator-erbium fiber amplifier MOPA or 2 micron Tm:YAG
Earth atmospheric methane	Nd laser pumped diode oscillator/seed OPA/OPO or Diode oscillator Er:YGG amplifier
Improved Earth gravity - Gravity Recovery And Climate Experiment 2 (GRACE-II)	Nd:YAG Monolithic NPRO or ?
Precision time transfer – improved Global Positioning System (GPS)	Fiber frequency comb ?

NASA Space Laser Technology

SUMMARY

1. Over the past two decades NASA has deployed diode, solid state and fiber lasers based instruments for new spacecraft systems and science discoveries.

1. A second generation of space laser instruments will benefit from further monolithic laser manufacturing techniques.

2. NASA needs US industry and University help in developing robust, monolithic high power lasers for future space laser instruments

Acknowledgement

The authors would like to thank

NASA ESTO;

NASA ASTID program;

GSFC IRAD program;

GSFC SBIR program

and the

Instrument and Science Teams of:

MOLA, ICESat/GLAS, Calipso, MLA, LOLA, ICESat-2, LIST SDT, ASCENDS, GRACE-FO, GRACE-II, LADEE, LLCD & LCRD

Satellite clock synchronization
Atomic Clock Ensemble in Space (ACES) on ISS in 2016 - European Space Agency

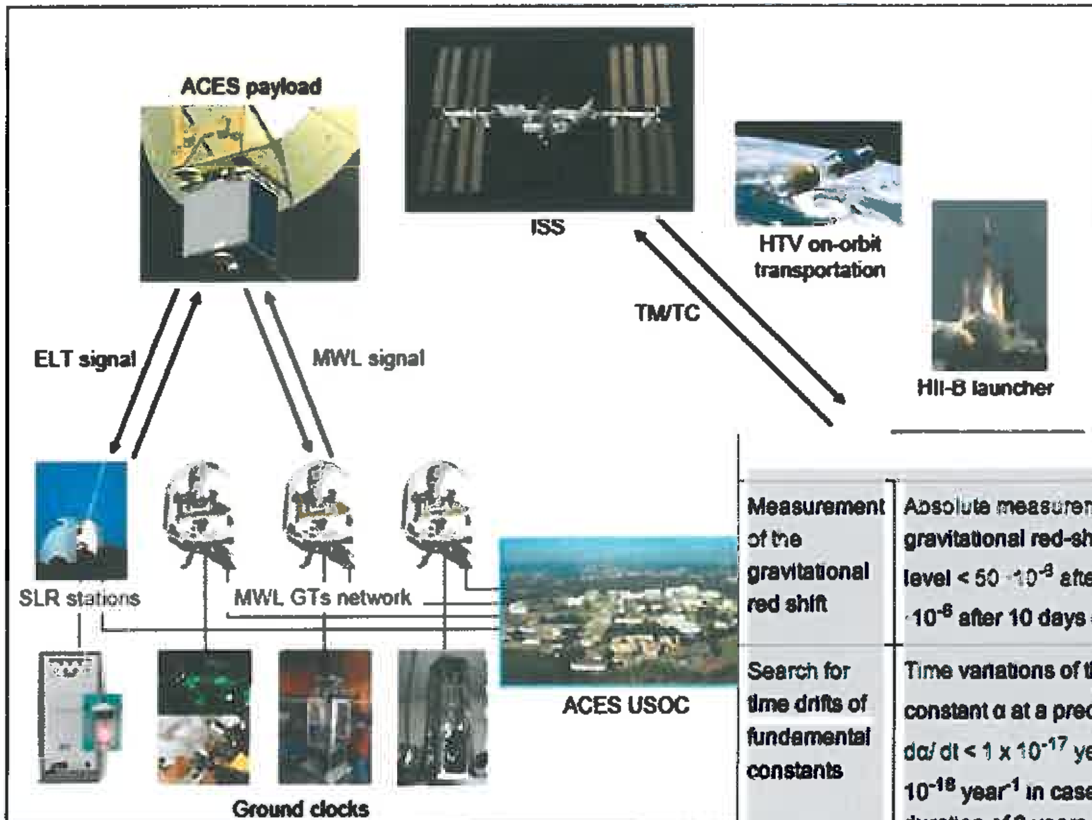

Figure 20: Overview of the ACES mission architecture (image credit: E

Fundamental Physics tests		
Measurement of the gravitational red shift	Absolute measurement of the gravitational red-shift at an uncertainty level < 50 $\cdot 10^{-6}$ after 300 s and < 2 $\cdot 10^{-6}$ after 10 days of integration time	Space-to-ground clock comparison at the 10^{-16} level, will yield a factor 35 improvement on previous measurements (GPA experiment).
Search for time drifts of fundamental constants	Time variations of the fine structure constant α at a precision level of α^{-1} $d\alpha/dt < 1 \times 10^{-17}$ year^{-1} down to 3 x 10^{-18} year^{-1} in case of a mission duration of 3 years	Optical clocks progress will allow clock-to-clock comparisons below the 10^{-17} level. Crossed comparisons of clocks based on different atomic elements will impose strong constraints on the time drifts of α, m_e/Λ_{QCD}, and m_u/Λ_{QCD}
Search for violations of special relativity	Search for anisotropies of the speed of light at the level $\delta c/c < 10^{-10}$	ACES results will improve present limits on the RMS parameter α based on fast ions spectroscopy and GPS satellites by one and two orders of magnitudes, respectively.

ELT (European Laser Timing)

PHARAO (Project d'Horloge Atomique à Refroidissement d'Atomes en Orbite): a laser-cooled cesium atomic clock